TECHNISCHE MECHANIK, Band 20, Heft 2, (2000), 147-157
Manuskripteingang: 25. November 1999

On Parametrically Excited Flexural Motion of an Extensible and Shearable Rod with a Heavy Attachment

S.J. Cull, R.W. Tucker, R.S. Tung, D.H. Hartley

A simple Cosserat model is used to explore the coupled planar flexural and axial vibrations of a slender rod clamped at one end with a heavy attached mass free to move at the other. By assuming that the inertia of the rod is small compared to that of the attached mass it is shown how the equations of motion reduce to a dynamical system. The effects of gravity on the rod can be incorporated within this framework and the linearised stability of the system discussed in terms of solutions to the Mathieu-Hill equation.

1 Introduction

The analysis of slender elastic structures under external forces and torques remains an active area of study. Although simplified models may capture aspects of axial, lateral or torsional linearised instabilities a unified model is necessary to properly appreciate the rich dynamical interactions between these modes and the non-linearities that inevitably limit the applicability of the simplest models. In this paper we explore the linear stability of small axial and lateral excitations of an extensible, shearable rod, clamped at one end with a heavy attachment at the other, using methods adopted in Tucker et al. (1999).

A rod is modelled in terms of space-curve with structure. This structure defines the relative orientation of neighbouring cross-sections along the rod. Specifying a unit vector (which may be identified with the normal to each cross-section) at each point along the line of centroids enables the state of flexure to be related to the angle between this vector and the tangent to the space-curve. Specifying a second vector orthogonal to the first vector (thereby placing it in the plane of the cross-section) can be used to encode the state of bending and twist along the rod. Thus a field of two mutually orthogonal unit vectors $\{\mathbf{d}_1(\sigma,\eta),\ \mathbf{d}_2(\sigma,\eta)\}$ along the rod provides three continuous dynamical degrees of freedom that, together with the continuous three degrees of freedom describing a space-curve relative to some arbitrary origin in space, define a simple Cosserat rod model.

In Tucker and Wang (1999b) it has been shown how a drill-string in a typical oil or gas rig may be described in terms of such a model. Supplemented with appropriate constitutive relations and boundary conditions the model can fully accommodate the modes of vibration that are traditionally associated with the motion of drill-strings in the engineering literature: namely axial motion along the length of the drill-string, torsional or rotational motion and transverse or lateral motion (Dunayevsky et al., 1993; Fear and Abbassian, 1994). This model is well suited to study numerical simulations that offer valuable guidance on the detection and control of destructive vibrational configurations (Tucker and Wang, 1999a). One of the drawbacks, however, of a direct numerical simulation of such a 3D model is the extensive computational time required to gain significant insights into the structure of the control space that determines the stability of the system. This can be particularly acute when, due to non-linearities in the equations of motion or (moving) boundary conditions, the evolution of the system becomes sensitive to initial conditions and parametric variations.

Novel approximations of the governing non-linear partial differential equations offer a means to explore the relevance of different parameter domains on the evolution of a direct numerical simulation. Even though recourse to further numerical analysis may be required the insights gained from such approximations prove invaluable when establishing initial conditions and parameter domains for a full 3D simulation. One may then investigate the limits of validity of an approximate solution. Within such limits such solutions offer an efficient computation scheme by comparison with a full numerical simulation and their analytic implications provide a useful complement to a purely computational understanding of such a complex phenomenon.

Inspired by Antman et al. (1998) a study of the dynamics of large amplitude flexural motion in the context of extensible and shearable drill-strings under gravity has begun, with a view to controlling the

onset of "snap-buckling" (Tucker et al., 1999). Antman et al. (1998) have provided general conditions on initial data that permit a certain approximation scheme for a simple Cosserat system to generate a solution that can move irregularly through a family of equilibrium states parametrised by time. In Tucker et al. (1999) we have shown that approximations in which the pde system is reduced to a non-linear ode system provide a useful guide to the behaviour of large flexural vibrations. By contrast in this paper attention is directed to the linearised stability of axial and planar flexural excitations of small amplitude. New approximation schemes are compared with direct numerical computations using the method of mapping at a period (Arnold, 1989) and for the first time within this context applied to the parametric amplification of extensible, shearable rods with weight.

Although this work has been motivated by the dynamics of drill strings it has implications for other systems. The analysis of recent precision experiments (Quinn et al., 1992; Speake et al., 1999) to measure the Newtonian gravitational coupling constant G using the motion of a compound pendulum suspended from alloy flexure strips needs to accommodate (low frequency) elastodynamic behaviour. With suitable modifications to boundary and damping conditions the results discussed below have relevance to such a system and should offer an important method to enhance the precision of such measurements.

2 The Simple Cosserat Model

In this section the basic equations of the simple Cosserat theory for a slender rod of unstressed length L_0 metres are briefly summarised and the dimensionless equations of motion and boundary conditions that are subsequently discussed are derived. Elements of the rod are labelled in terms of the Lagrangian coordinate $0 \leq s \leq L_0$ at time t.

In terms of external force $\mathbf{f}$ and torque $\mathbf{l}$ densities the dimensionless equations of motion (Antman, 1991; Tucker and Wang, 1999b) for the rod are (with $\mathbf{d}_3 = \mathbf{d}_1 \times \mathbf{d}_2$ and $k = 1, 2, 3$):

$$\begin{aligned}
\ddot{\mathbf{R}}(\sigma,\eta) &= \mathbf{n}'(\sigma,\eta) - g\mathbf{k} + \mathbf{f}(\sigma,\eta) && (1)\\
((\rho\mathbf{I})(\mathbf{w}(\sigma,\eta)))_\eta &= \mathbf{m}'(\sigma,\eta) + \kappa(\mathbf{R}'(\sigma,\eta) \times \mathbf{n}(\sigma,\eta)) + \mathbf{l}(\sigma,\eta) && (2)\\
\mathbf{d}_k{}'(\sigma,\eta) &= \mathbf{u}(\sigma,\eta) \times \mathbf{d}_k(\sigma,\eta) && (3)\\
\dot{\mathbf{d}}_k(\sigma,\eta) &= \mathbf{w}(\sigma,\eta) \times \mathbf{d}_k(\sigma,\eta) && (4)\\
\mathbf{R}_\sigma(\sigma,\eta) &= \mathbf{v}(\sigma,\eta) && (5)
\end{aligned}$$

where $\sigma = s/L_0$, $\dot{\mathbf{R}} = \partial_\eta \mathbf{R}, \mathbf{R}' = \partial_\sigma \mathbf{R}$ etc., κ is the dimensionless constant $(E\mathcal{A})(\sigma)L_0^2\rho_0/(G(\hat{I}_{11} + \hat{I}_{22}))$ in terms of Young's modulus E for the rod, $\mathcal{A}(\sigma)$ its cross-sectional area, ρ_0 its uniform density and G its shear modulus. The weight of the rod (extracted from the body force density $\mathbf{f}$) is encoded into the dimensionless parameter $g = \hat{g}\rho_0 L_0/E$ where $\hat{g}$ is the acceleration due to gravity and the evolution of the system is given in terms of time t by the dimensionless variable $\eta = ct/L_0$ where $c = \sqrt{E/\rho_0}$. The vector

$$\mathbf{w}(\sigma,\eta) = w_1(\sigma,\eta)\mathbf{d}_1(\sigma,\eta) + w_2(\sigma,\eta)\mathbf{d}_2(\sigma,\eta) + w_3(\sigma,\eta)\mathbf{d}_3(\sigma,\eta) \quad (6)$$

denotes the local angular velocity of the rod . The dimensionless contact force $\mathbf{n}(\sigma,\eta)$ and torque $\mathbf{m}(\sigma,\eta)$ vectors

$$\begin{aligned}
\mathbf{n}(\sigma,\eta) &= n_1(\sigma,\eta)\mathbf{d}_1(\sigma,\eta) + n_2(\sigma,\eta)\mathbf{d}_2(\sigma,\eta) + n_3(\sigma,\eta)\mathbf{d}_3(\sigma,\eta) && (7)\\
\mathbf{m}(\sigma,\eta) &= m_1(\sigma,\eta)\mathbf{d}_1(\sigma,\eta) + m_2(\sigma,\eta)\mathbf{d}_2(\sigma,\eta) + m_3(\sigma,\eta)\mathbf{d}_3(\sigma,\eta) && (8)
\end{aligned}$$

are related to the dimensionless strain vectors $\mathbf{v}(\sigma,\eta)$ and $\mathbf{u}(\sigma,\eta)$

$$\begin{aligned}
\mathbf{v}(\sigma,\eta) &= v_1(\sigma,\eta)\mathbf{d}_1(\sigma,\eta) + v_2(\sigma,\eta)\mathbf{d}_2(\sigma,\eta) + v_3(\sigma,\eta)\mathbf{d}_3(\sigma,\eta) && (9)\\
\mathbf{u}(\sigma,\eta) &= u_1(\sigma,\eta)\mathbf{d}_1(\sigma,\eta) + u_2(\sigma,\eta)\mathbf{d}_2(\sigma,\eta) + u_3(\sigma,\eta)\mathbf{d}_3(\sigma,\eta) && (10)
\end{aligned}$$

by the the classical Kirchoff constitutive relations:

$$\mathbf{n}(\sigma,\eta) = \chi\mathbf{v}(\sigma,\eta) + ((1-\chi)v_3(\sigma,\eta) - 1)\mathbf{d}_3(\sigma,\eta) \quad (11)$$

$$\mathbf{m}(\sigma,\eta) = \frac{1}{\beta}\mathbf{u}(\sigma,\eta) + (1-\frac{1}{\beta})u_3(\sigma,\eta)\mathbf{d}_3(\sigma,\eta) \tag{12}$$

where the dimensionless parameter $\chi = G/E$ is expressed in terms of the ratio of shear to (Young's) modulus of elasticity, and $\beta = G(\hat{I}_{11}+\hat{I}_{22})/(E\hat{I}_{11})$, is defined by a set of reduced (dimensionless) inertia components of the rod. The $\hat{I}_{ij}$ are the components of the rod "inertia tensor", $(\rho\hat{\mathbf{I}})$, with respect to the local director frame $\{\mathbf{d}_j\}$. For a cylindrical rod with an annular cross section, outer radius r_O and inner radius r_I the non zero components of $\hat{I}_{ij}$ are

$$\hat{I}_{11} = \hat{I}_{22} = \pi\rho_0(r_O^4 - r_I^4)/4$$

$$\hat{I}_{33} = \pi\rho_0(r_O^4 - r_I^4)/2$$

The triad $\{\mathbf{i},\mathbf{j},\mathbf{k}\}$ will denote a right-handed global orthonormal basis for vectors in space, oriented so that $\mathbf{k}$ points vertically upwards and the upper end of the rod is attached to the origin of this basis. At $\sigma = 0$ the variables $\mathbf{R}, \mathbf{w}$ satisfy the equation of motion of a rigid body with heavy effective reduced mass μ_0 and effective reduced inertia $\mathbf{J}_0(\eta)$,

$$\mu_0\ddot{\mathbf{R}}_0(\eta) = \mathbf{n}_0(\eta) - \mu_0 g\mathbf{k} + \mathbf{f}_0(\eta) \qquad \partial_\eta[\mathbf{J}_0(\eta)\cdot\mathbf{w}_0(\eta)] = \mathbf{m}(\sigma,\eta)_0(\eta) + \mathbf{l}_0(\eta) \tag{13}$$

where $\mathbf{R}_0(\eta) = \mathbf{R}(0,\eta), \mathbf{n}_0(\eta) = \mathbf{n}(0,\eta), \mathbf{m}_0(\eta) = \mathbf{m}(0,\eta), \mathbf{w}_0(\eta) = \mathbf{w}(0,\eta)$. Similarly at $\sigma = 1$, these variables satisfy the equation of motion of a rigid body with heavy effective reduced mass μ_1 and effective reduced inertia $\mathbf{J}_1(\eta)$:

$$\mu_1\ddot{\mathbf{R}}_1(\eta) = -\mathbf{n}_1(\eta) - \mu_1 g\mathbf{k} + \mathbf{f}_1(\eta) \qquad \partial_\eta[\mathbf{J}_1(\eta)\cdot\mathbf{w}_1(\eta)] = -\mathbf{m}(\sigma,\eta)_1(\eta) + \mathbf{l}_1(\eta) \tag{14}$$

where $\mathbf{R}_1(\eta) = \mathbf{R}(1,\eta), \mathbf{n}_1(\eta) = \mathbf{n}(1,\eta), \mathbf{m}_1(\eta) = \mathbf{m}(1,\eta), \mathbf{w}_1(\eta) = \mathbf{w}(1,\eta)$. We further consider planar flexural modes with ($\mathbf{f} = \mathbf{l} = 0$, $\mathbf{f}_1 = 0 = \mathbf{l}_1$) and an approximation where the left-hand sides of equations (1) and (2) may be neglected at all time compared with the forces and torques on the right-hand sides. This approximation (Antman et al., 1998; Tucker et al., 1999) implies that the dynamical motion at an end of the rod dominates the forces and torques that drive the system. Under these circumstances equation (1) may be readily integrated with respect to σ

$$\mathbf{n}(\sigma,\eta) = g(\sigma-1)\mathbf{k} + \mathbf{n}_1(\eta) = g\sigma\mathbf{k} + \mathbf{n}_0(\eta) \tag{15}$$

while equation (2) becomes

$$\mathbf{m}'(\sigma,\eta) = -\kappa\mathbf{R}'(\sigma,\eta)\times\mathbf{n}(\sigma,\eta) \tag{16}$$

As in Tucker et al. (1999) the special case $\chi = 1$ is explored:

$$\mathbf{n}(\sigma,\eta) = \mathbf{v}(\sigma,\eta) - \mathbf{d}_3(\sigma,\eta) \qquad \mathbf{m}(\sigma,\eta) = \tfrac{1}{\beta}\mathbf{u}(\sigma,\eta) + (1-\tfrac{1}{\beta})u_3\mathbf{d}_3(\sigma,\eta) \tag{17}$$

With these constitutive relations the rod can undergo extension and shear. It follows that

$$\mathbf{R}'(\sigma,\eta) = \mathbf{n}_1(\eta) + g(\sigma-1)\mathbf{k} + \mathbf{d}_3(\sigma,\eta) \tag{18}$$

$$\kappa^{-1}\mathbf{m}'(\sigma,\eta) = -\mathbf{R}'(\sigma,\eta)\times\mathbf{n}(\sigma,\eta) = \mathbf{n}_1(\eta)\times\mathbf{d}_3(\sigma,\eta) + g(\sigma-1)\mathbf{k}\times\mathbf{d}_3(\sigma,\eta) \tag{19}$$

$$\mathbf{d}_3'(\sigma,\eta) = \mathbf{u}(\sigma,\eta)\times\mathbf{d}_3(\sigma,\eta) = \beta\mathbf{m}(\sigma,\eta)\times\mathbf{d}_3(\sigma,\eta) \tag{20}$$

$$\mathbf{d}_1'(\sigma,\eta) = \mathbf{u}(\sigma,\eta)\times\mathbf{d}_1(\sigma,\eta) = \beta\mathbf{m}(\sigma,\eta)\times\mathbf{d}_1(\sigma,\eta) + (1-\beta)m_3\mathbf{d}_3(\sigma,\eta)\times\mathbf{d}_1(\sigma,\eta) \tag{21}$$

$$\mathbf{d}_2'(\sigma,\eta) = \mathbf{u}(\sigma,\eta)\times\mathbf{d}_2(\sigma,\eta) = \beta\mathbf{m}(\sigma,\eta)\times\mathbf{d}_2(\sigma,\eta) + (1-\beta)m_3\mathbf{d}_3(\sigma,\eta)\times\mathbf{d}_2(\sigma,\eta) \tag{22}$$

We consider solutions of the form:

$$\begin{aligned}\mathbf{R}(\sigma,\eta) &= X(\sigma,\eta)\mathbf{i} + Z(\sigma,\eta)\mathbf{k}\\ \mathbf{d}_1(\sigma,\eta) &= -\cos\theta(\sigma,\eta)\mathbf{i} + \sin\theta(\sigma,\eta)\mathbf{k}\\ \mathbf{d}_2(\sigma,\eta) &= \mathbf{j}\\ \mathbf{d}_3(\sigma,\eta) &= -\sin\theta(\sigma,\eta)\mathbf{i} - \cos\theta(\sigma,\eta)\mathbf{k}\end{aligned} \tag{23}$$

It follows from equation (16) that:

$$\begin{aligned}\mathbf{w}(\sigma,\eta) &= \dot{\theta}(\sigma,\eta)\,\mathbf{j}\\ \mathbf{u}(\sigma,\eta) &= \theta'(\sigma,\eta)\,\mathbf{j}\\ \mathbf{m}(\sigma,\eta) &= \tfrac{1}{\beta}\theta'(\sigma,\eta)\,\mathbf{j}\\ \mathbf{n}_1(\eta) &= n_{1x}(\eta)\,\mathbf{i} + n_{1z}(\eta)\,\mathbf{k}\end{aligned} \tag{24}$$

Introduce new variables $A(\eta), \gamma(\eta)$ in place of $n_{1x}(\eta), n_{1z}(\eta)$ by writing

$$\mathbf{n}_1(\eta) = -(\beta\kappa)^{-1}A(\eta)^2(\sin\gamma(\eta)\mathbf{i} + \cos\gamma(\eta)\mathbf{k}) \tag{25}$$

(without loss of generality, and set $A(\eta) \geq 0$ and $-\pi \leq \gamma(\eta) \leq \pi$). In the following section a cylindrical rod with an annular cross section is chosen so that $\beta = 2$ with $\chi = 1$. By differentiating $\mathbf{m}(\sigma,\eta) = \frac{1}{\beta}\theta'\,\mathbf{j}$ with respect to σ and equating it to equation (16) $\theta(\sigma,\eta)$ is found to satisfy

$$\begin{aligned}\theta''(\sigma,\eta) &= -2\kappa[n_{1z}(\eta)\sin\theta(\sigma,\eta) - n_{1x}(\eta)\cos\theta(\sigma,\eta)] - 2\kappa g(\sigma-1)\sin\theta(\sigma,\eta)\\ &= A(\eta)^2\sin(\theta(\sigma,\eta) - \gamma(\eta)) - 2\kappa g(\sigma-1)\sin\theta(\sigma,\eta)\end{aligned} \tag{26}$$

A light rod is defined by setting $g = 0$. With this further simplification one integrates equation (18) using equations (23) to get

$$\mathbf{R}(\sigma,\eta) = \mathbf{R}_0(\eta) - (2\kappa)^{-1}\sigma A(\eta)^2(\sin\gamma(\eta)\mathbf{i} + \cos\gamma(\eta)\mathbf{k}) - \int_0^\sigma d\sigma'(\sin\theta(\sigma',\eta)\mathbf{i} + \cos\theta(\sigma',\eta)\mathbf{k}) \tag{27}$$

The rod is assumed clamped at the origin ($\sigma = 0$) with $\mathbf{R}(0,\eta) = 0$, $\mathbf{d}_1(0,\eta) = -\mathbf{i}, \mathbf{d}_2(0,\eta) = \mathbf{j}, \mathbf{d}_3(0,\eta) = -\mathbf{k}$, and the attached mass at $\sigma = 1$ has zero rotary inertia, $\mathbf{J}_1(\eta) = 0$. It follows from equations (23) that $\theta_0(\eta) = 0$ while equations (14) and (24) imply $\theta_1'(\eta) = 0$. Thus together with equation (26) the boundary value problem is

$$\theta''(\sigma,\eta) - A(\eta)^2\sin(\theta(\sigma,\eta) - \gamma(\eta)) = 0 \tag{28}$$

$$\theta_0(\eta) = 0 \qquad\qquad \theta_1'(\eta) = 0 \tag{29}$$

3 Flexural Excitations with $\chi = 1$ and $g = 0$

Restricting attention to small flexural excitations with $\theta \ll 1$, equation (28) becomes:

$$\theta''(\sigma,\eta) - (A(\eta)^2\cos\gamma(\eta))\theta(\sigma,\eta) = -A(\eta)^2\sin\gamma(\eta) \tag{30}$$

The solution for $\theta(\sigma,\eta)$ satisfying the above boundary conditions, using Green's function methods described e.g. in Collatz (1986), is

$$\theta(\sigma,\eta) = -\frac{A(\eta)^2\sin\gamma(\eta)}{B(\eta)^2}(1 - \tan B(\eta)\sin(B(\eta)\sigma) - \cos(B(\eta)\sigma)) \tag{31}$$

where the complex variable $B(\eta) = A(\eta)\sqrt{-\cos\gamma(\eta)}$. From equation (27)

$$\mathbf{R}(1,\eta) = -(2\kappa)^{-1}A(\eta)^2(\sin\gamma(\eta)\mathbf{i} + \cos\gamma(\eta)\mathbf{k}) - \int_0^1 d\sigma'(\sin\theta(\sigma',\eta)\mathbf{i} + \cos\theta(\sigma',\eta)\mathbf{k}) \tag{32}$$

$$= X_1(\eta)\mathbf{i} + Z_1(\eta)\mathbf{k} \tag{33}$$

so with $\theta \ll 1$ in the integrand above, we have

$$\int_0^1 d\sigma'\theta(\sigma') = -\frac{A(\eta)^2\sin\gamma(\eta)}{B(\eta)^2}\left(1 - \frac{\tan(B(\eta))}{B(\eta)}\right) \tag{34}$$

and since

$$\lim_{B\to 0}\frac{1}{B(\eta)^2}\left(1 - \frac{\tan(B(\eta))}{B(\eta)}\right) = -\frac{1}{3} \tag{35}$$

$$X_1(\eta) = -(2\kappa)^{-1}A(\eta)^2\sin\gamma(\eta) + \frac{A(\eta)^2\sin\gamma(\eta)}{B(\eta)^2}\left(1 - \frac{\tan(B(\eta))}{B(\eta)}\right) \tag{36}$$

$$Z_1(\eta) = -(2\kappa)^{-1}A(\eta)^2\cos\gamma(\eta) - 1 \tag{37}$$

The evolution equation

$$\mu_1\ddot{\mathbf{R}}_1(\eta) = -\mathbf{n}_1(\eta) = (2\kappa)^{-1}A(\eta)^2(\sin\gamma(\eta)\mathbf{i} + \cos\gamma(\eta)\mathbf{k}) \tag{38}$$

can then be expressed in terms of $X_1(\eta)$ and $Z_1(\eta)$:

$$\mu_1\ddot{X}_1(\eta) = -X_1(\eta)\left(1 - \frac{2\kappa}{B(\eta)^2}\left(1 - \frac{\tan B(\eta)}{B(\eta)}\right)\right)^{-1} \tag{39}$$

$$\mu_1\ddot{Z}_1(\eta) = -1 - Z_1(\eta) \tag{40}$$

where, from equation (37), $B(\eta) = \sqrt{2\kappa}\sqrt{1 + Z_1(\eta)}$. The general solution of equation (40), with initial values $Z_1(0)$ and $\dot{Z}_1(0)$, is

$$Z_1(\eta) = -1 + (Z_1(0) + 1)\cos(\frac{\eta}{\sqrt{\mu_1}}) + \sqrt{\mu_1}\dot{Z}_1(0)\sin(\frac{\eta}{\sqrt{\mu_1}}) \tag{41}$$

From equations (37) and (41) $B(\eta)^2$ is determined by these initial conditions $Z_1(\eta)$, $\dot{Z}_1(\eta)$:

$$B(\eta)^2 = 2\kappa\left[\left(1 + Z_1(0)\right)\cos(\frac{\eta}{\sqrt{\mu_1}}) + \sqrt{\mu_1}\dot{Z}_1(0)\sin(\frac{\eta}{\sqrt{\mu_1}})\right] \tag{42}$$

$$= 2\kappa H\cos(\frac{\eta}{\sqrt{\mu_1}} + \tau_0) \tag{43}$$

where $H = \sqrt{\left(1 + Z_1(0)\right)^2 + \mu_1\left(\dot{Z}_1(0)\right)^2}$ and

$$\tan\tau_0 = -\sqrt{\mu_1}\frac{\dot{Z}_1(0)}{1 + Z_1(0)} \tag{44}$$

Equation (39) may describe parametric excitations via the periodic function $B(\eta) = B(\eta + 2\pi\sqrt{\mu_1})$. Since the dynamics of $B(\eta)$ is determined by the extensible motion $Z_1(\eta)$ there exists the possibility of auto-parametric excitation and internal resonance in the system. The parametric "stiffness" in equation (40) can become unbounded as $B(\eta)$ approaches $\pi/2$ from below and it is difficult to solve this equation

analytically. Given the possibility of unbounded solutions its behaviour for $\kappa H \ll 1$ is explored, since from equation (43) one may then use the approximation $|B(\eta)^2| \ll 1$. For the special initial values $Z_1(0) = 1$, $\dot{Z}_1(0) = 0$, one has $B(\eta) = 0$ and equation (39) reduces to

$$\ddot{X}_1(\eta) + \frac{1}{\mu_1}\left(1 + \frac{2}{3}\kappa\right)^{-1} X_1(\eta) = 0 \tag{45}$$

with oscillatory solutions. With general initial conditions for the $Z_1(\eta)$ motion but $\kappa H \ll 1$

$$\left(1 - \frac{2\kappa}{B(\eta)^2}\left(1 - \frac{\tan(B(\eta))}{B(\eta)}\right)\right)^{-1} \tag{46}$$

$$= \left(1 + \frac{2}{3}\kappa\right)^{-1} - \left(1 + \frac{2}{3}\kappa\right)^{-2} \frac{4}{15}\kappa B(\eta)^2 + O(B^4) \tag{47}$$

$$= \left(1 + \frac{2}{3}\kappa\right)^{-1} - \left(1 + \frac{2}{3}\kappa\right)^{-2} \frac{8}{15}\kappa^2 H \cos\left(\frac{\eta}{\sqrt{\mu_1}} + \tau_0\right) + O(B^4) \tag{48}$$

Equation (39) may be approximated by the Mathieu-Hill equation

$$\ddot{X}_1(\eta) + \left[\frac{1}{\mu_1}\left(1 + \frac{2}{3}\kappa\right)^{-1} - \left(1 + \frac{2}{3}\kappa\right)^{-2} \frac{8\kappa^2}{15\mu_1} H \cos\left(\frac{\eta}{\sqrt{\mu_1}} + \tau_0\right)\right] X_1(\eta) = 0 \tag{49}$$

With $T = \frac{\eta}{\sqrt{\mu_1}} + \tau_0$ the equation can be written in standard form:

$$\frac{d^2}{dT^2}\hat{X} + [a - b\cos T]\,\hat{X} = 0 \tag{50}$$

where

$$X_1(\eta) = \hat{X}_1\left(\frac{\eta}{\sqrt{\mu_1}} + \tau_0\right) \tag{51}$$

$$a = \left(1 + \frac{2}{3}\kappa\right)^{-1} \tag{52}$$

$$b = \left(1 + \frac{2}{3}\kappa\right)^{-2} \frac{8\kappa^2}{15} H \tag{53}$$

Equation (50) exhibits unbounded oscillations for certain values of a and b. The stability domains follow from a standard analysis of the Mathieu-Hill equation (Newland, 1989) and are displayed in Figure 1, where the stable regions are shaded. Since $b > 0$, $0 < a < 1$, there exist domains of unstable flexural motion in this limit. One such region is bounded by the curve labelled "approximate" in Figure 2 in terms of κ and H where

$$\kappa = \frac{3}{2}\left(\frac{1}{a} - 1\right) \tag{54}$$

$$H = \frac{5}{6}\left(\frac{b}{(a-1)^2}\right) \tag{55}$$

Since

$$|B(\eta)^2| = 2\kappa\sqrt{\left(1 + Z_1(0)\right)^2 + \mu_1\left(\dot{Z}_1(0)\right)^2}\,|\cos T| = 2\kappa H\,|\cos T| \tag{56}$$

stability criteria based on parameters having values that lie in the region below the hyperbola $\kappa H = 1/2$ and above the κ axis in Figure 2 are consistent with the small $|B(\eta)^2|$ approximation. Parameters that lie in the domain between the curves that intersect on the κ-axis at $\kappa = 4.5$ gives rise to unstable motion for any value of H determined by the initial values of $Z_1(\eta)$ and $\dot{Z}_1(\eta)$ with $B(\eta) \neq 0$.

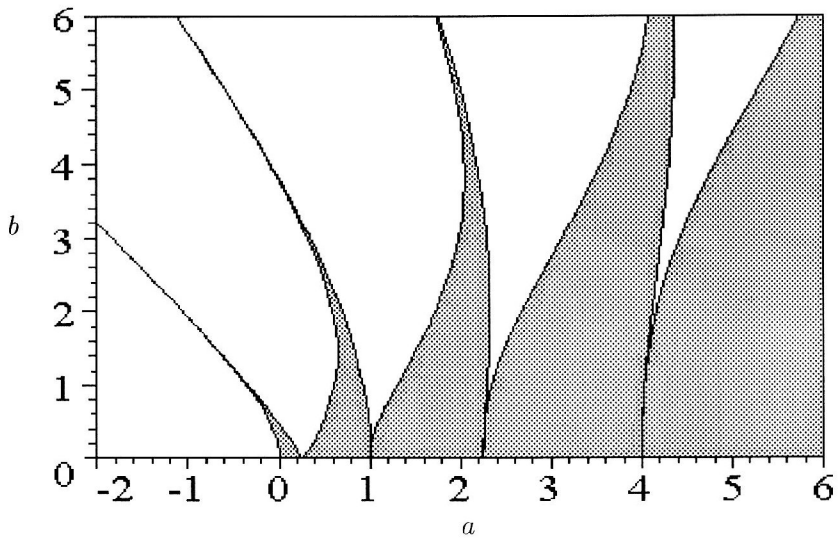

Figure 1: Mathieu-Hill stability diagram showing shaded stable regions in the a-b plane associated with equation (50).

One may solve equation (39) numerically without recourse to the small κH approximation. The motion $\mathbf{R}(\sigma,\eta)$ of the rod in space is then determined from the relations:

$$X(\sigma,\eta) = n_x(\eta)\sigma + \frac{n_x(\eta)}{n_z(\eta)}\left(\frac{\sigma B(\eta)\cos B(\eta) - \sin B(\eta) + \sin((1-\sigma)B(\eta))}{B(\eta)\cos(B(\eta))}\right) \tag{57}$$

$$Z(\sigma,\eta) = Z_1(\eta)\sigma \tag{58}$$

where $n_x(\eta) = -\mu_1\ddot{X}_1(\eta)$, $n_z(\eta) = -\mu_1\ddot{Z}_1(\eta) = Z_1(\eta) + 1$. The curve labelled "direct" in Figure 2 shows the result of the stability analysis performed by direct numerical computation using the method of mapping at a period (Arnold, 1989) without the small κH approximation. Below the hyperbola agreement is good.

4 Flexural Excitations with $\chi = 1$ and $g \neq 0$

In the previous section the weight of the rod has been neglected. In this section the effect of the rod's weight on the excitation of small flexural excitations is explored. By differentiating the equation $\mathbf{m}(\sigma,\eta) = \frac{1}{\beta}\theta'\mathbf{j}$ in section (2) with respect to σ, and equating it to equation (16) yields

$$\theta''(\sigma,\eta) = -\beta\kappa([g(\sigma-1) + n_{1z}(\eta)]\sin\theta(\sigma,\eta) - n_{1x}(\eta)\cos\theta(\sigma,\eta)) \tag{59}$$

With $g = 0$ this equation subject to the boundary conditions (29) has been analysed in terms of elliptic integrals (Tucker et al., 1999). To progress when $g \neq 0$ assume small flexural deflections and write the above equation

$$\theta''(\sigma,\eta) + \beta\kappa[g(\sigma-1) + n_{1z}(\eta)]\theta(\sigma,\eta) = \beta\kappa n_{1x}(\eta) \tag{60}$$

subject to the boundary conditions (29). Linearly independent solutions to the homogeneous equation are

$$\theta_1(\sigma,\eta) = \mathrm{Ai}\,(\Psi(\sigma,\eta)) \qquad \theta_2(\sigma,\eta) = \mathrm{Bi}\,(\Psi(\sigma,\eta)) \tag{61}$$

where Ai and Bi are the Airy A and Airy B functions and

$$\Psi(\sigma,\eta) = (\beta\kappa g)^{\frac{1}{3}}\left(-\sigma + 1 - \frac{n_{1z}(\eta)}{g}\right) \tag{62}$$

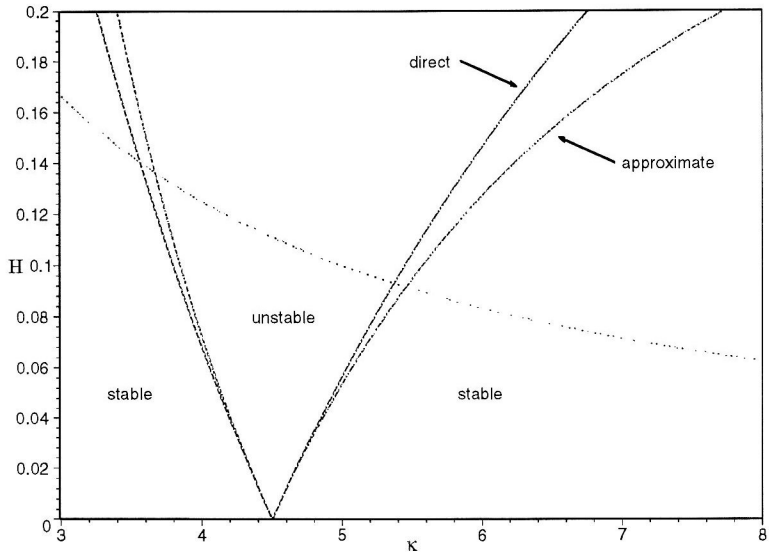

Figure 2: Stability diagram showing the stable regions in the κ-H plane associated with equation (39). The hyperbolic line is $\kappa H = 1/2$, with the region $\kappa H < 1/2$ corresponding to $|B^2| < 1$. The curve labelled "direct" shows the result of direct numerical calculations with equation (39), while the curve labelled "approximate" corresponds to the Mathieu-Hill equation (50).

Using linear combinations of the solutions (61) one may write down the solution $\theta_L(\sigma,\eta)$ of the homogeneous equation satisfying the boundary condition $\theta_0(\eta) = 0$, and similarly the solution $\theta_R(\sigma,\eta)$ satisfying the boundary condition $\theta_1'(\eta) = 0$:

$$\theta_L(\sigma,\eta) = -\frac{\mathrm{Bi}\,(\Psi(0,\eta))}{\mathrm{Ai}\,(\Psi(0,\eta))}\,\mathrm{Ai}\,(\Psi(\sigma,\eta)) + \mathrm{Bi}\,(\Psi(\sigma,\eta)) \tag{63}$$

$$\theta_R(\sigma,\eta) = -\frac{\mathrm{Bi}\,(1,\Psi(1,\eta))}{\mathrm{Ai}\,(1,\Psi(1,\eta))}\,\mathrm{Ai}\,(\Psi(\sigma,\eta)) + \mathrm{Bi}\,(\Psi(\sigma,\eta)) \tag{64}$$

where

$$\mathrm{Ai}\,(1,\sigma) = \frac{d}{d\sigma}\,\mathrm{Ai}\,(\sigma) \tag{65}$$

$$\mathrm{Bi}\,(1,\sigma) = \frac{d}{d\sigma}\,\mathrm{Bi}\,(\sigma) \tag{66}$$

The Wronskian of the functions θ_L and θ_R is a constant in σ

$$W_\theta(\eta) = (\beta\kappa g)^{\frac{1}{3}}\left(\frac{\mathrm{Bi}\,(\Psi(0,\eta))}{\mathrm{Ai}\,(\Psi(0,\eta))} - \frac{\mathrm{Bi}\,(1,\Psi(1,\eta))}{\mathrm{Ai}\,(1,\Psi(1,\eta))}\right)\pi^{-1} \tag{67}$$

The solution to equation (60) satisfying the boundary conditions (29) is:

$$\theta(\sigma,\eta) = \frac{\beta\kappa n_{1x}(\eta)}{W_\theta}\left(\theta_L(\sigma,\eta)\int_\sigma^1 \theta_R(\xi,\eta)\,d\xi + \theta_R(\sigma,\eta)\int_0^\sigma \theta_L(\xi,\eta)\,d\xi\right) \tag{68}$$

With $\chi = 1$, one integrates equation (18) using equation (23) to get

$$X(\sigma,\eta) = \sigma n_{1x}(\eta) - \int_0^\sigma \theta(\tilde{\sigma},\eta)\,d\tilde{\sigma} \tag{69}$$

$$Z(\sigma,\eta) = \frac{g}{2}(\sigma^2 - 2\sigma) + \sigma n_{1z}(\eta) - \sigma \tag{70}$$

At $\sigma = 1$ the force boundary condition in equations (14) with $\mathbf{f}_1 = 0$ gives

$$\mu_1 \ddot{X}_1(\eta) = -n_{1x}(\eta) \tag{71}$$

$$\mu_1 \ddot{Z}_1(\eta) = -n_{1z}(\eta) - \mu_1 g \tag{72}$$

and substituting $\sigma = 1$ in equation (70) gives

$$n_{1z}(\eta) = Z_1(\eta) + \frac{g}{2} + 1 \tag{73}$$

Substituting the above into equation (72) yields

$$\mu_1 \ddot{Z}_1(\eta) = -1 - \left(\mu_1 + \frac{1}{2}\right) g - Z_1(\eta) \tag{74}$$

which, with the initial values $Z_1(0)$ and $\dot{Z}_1(0)$, gives the solution

$$\begin{aligned} Z_1(\eta) = -1 - \left(\mu_1 + \frac{1}{2}\right) g + \sqrt{\mu_1}\dot{Z}_1(0) \sin\left(\frac{\eta}{\sqrt{\mu_1}}\right) \\ + \left(Z_1(0) + 1 + \left(\mu_1 + \frac{1}{2}\right) g\right) \cos\left(\frac{\eta}{\sqrt{\mu_1}}\right) \end{aligned} \tag{75}$$

With

$$\hat{\theta}(\sigma, \eta) = \frac{\theta(\sigma, \eta)}{n_{1x}(\eta)} \tag{76}$$

and $\sigma = 1$ in equation (69):

$$X_1(\eta) = n_{1x}(\eta) \left[1 - \int_0^1 \hat{\theta}(\sigma, \eta)\, d\sigma\right] \tag{77}$$

Hence equation (71) becomes

$$\mu_1 \ddot{X}_1(\eta) = \left[\int_0^1 \hat{\theta}(\sigma, \eta)\, d\sigma - 1\right]^{-1} X_1(\eta) \tag{78}$$

With $\epsilon = \beta\kappa g << 1$ a series expansion of $\hat{\theta}$, from equations (76) and (68) is

$$\begin{aligned} \hat{\theta}(\sigma, \eta) = \frac{1}{2}\beta\kappa\sigma^2 - \beta\kappa\sigma + \beta\kappa \left[\frac{1}{8}\sigma - \frac{1}{6}\sigma^3 + \frac{1}{8}\sigma^4 - \frac{1}{40}\sigma^5 \right. \\ \left. - \left(\frac{1}{3}\sigma - \frac{1}{6}\sigma^3 + \frac{1}{24}\sigma^4\right) \frac{n_{1z}(\eta)}{g}\right] \epsilon \end{aligned} \tag{79}$$

to first order in ϵ. It follows that

$$\left[\int_0^1 \hat{\theta}(\sigma, \eta)\, d\sigma - 1\right]^{-1} = -\frac{1}{(1 + \frac{1}{3}\beta\kappa)} + \frac{\frac{2}{15}\frac{\beta\kappa n_{1z}(\eta)}{g} - \frac{1}{24}\beta\kappa}{(1 + \frac{1}{3}\beta\kappa)^2}\epsilon \tag{80}$$

to this order. Substituting $Z_1(\eta)$ in equation (73) gives

$$n_{1z}(\eta) = -\mu_1 g + \hat{H} \cos\left(\frac{\eta}{\sqrt{\mu_1}} + \hat{\tau}_0\right) \tag{81}$$

where

$$\hat{H} = \sqrt{\left(1 + Z_1(0) + \left(\mu_1 + \frac{1}{2}\right) g\right)^2 + \mu_1 \dot{Z}_1(0)^2} \tag{82}$$

$$\tan \hat{\tau}_0 = -\frac{\sqrt{\mu_1}\dot{Z}_1(0)}{1 + Z_1(0) + \left(\mu_1 + \frac{1}{2}\right) g} \tag{83}$$

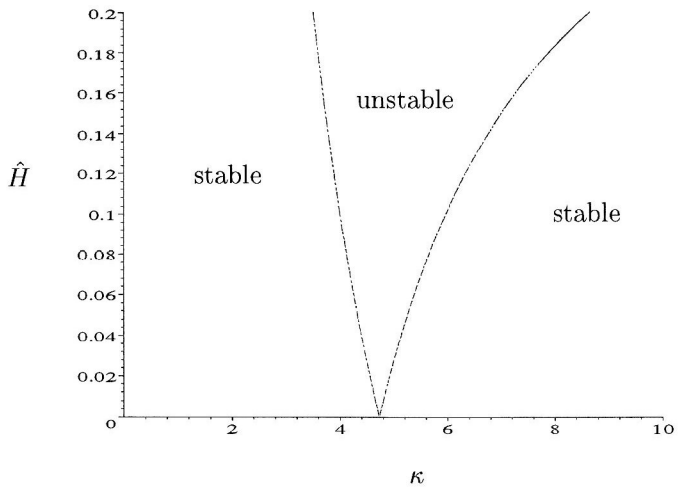

Figure 3: Stability diagram showing stable and unstable regions in the κ-$\hat{H}$ plane associated with equation (84) for $\beta = 2$, $\mu_1 = 1$, and $g = 0.01$.

Using equation (81) equation (78) is to first order in ϵ a form of the Mathieu-Hill equation. With $X_1(\eta) = \mathcal{X}_1(\hat{T})$ and $\hat{T} = \frac{\eta}{\sqrt{\mu_1}} + \hat{\tau}_0$, it can be expressed in the standard form:

$$\ddot{\mathcal{X}}_1(\hat{T}) + [\hat{a} - \hat{b}\cos\hat{T}]\mathcal{X}_1(\hat{T}) = 0 \tag{84}$$

with

$$\hat{a} = \left(1 + \frac{1}{3}\beta\kappa\right)^{-1} + \left(1 + \frac{1}{3}\beta\kappa\right)^{-2}\left(\frac{1}{8} + \frac{2}{5}\mu_1\right)\frac{\beta^2\kappa^2 g}{3} \tag{85}$$

$$\hat{b} = \left(1 + \frac{1}{3}\beta\kappa\right)^{-2}\frac{2\beta^2\kappa^2}{15}\hat{H} \tag{86}$$

As before equation (84) exhibits instabilities for certain values of $\hat{a}$ and $\hat{b}$. The stability domains follow from Figure 1, with a and b replaced by $\hat{a}$ and $\hat{b}$ respectively. We plot these stability domains in the κ-$\hat{H}$ plane, with $\beta = 2$, $\mu_1 = 1$, and $g = 0.01$, in figure 3.

5 Conclusions

A simple Cosserat model has been used to explore the coupled axial and planar flexural excitations of a rod clamped at one end with a heavy attached mass free to move at the other. The rod exhibits both extension and shear and a series of approximations permit the motion of small planar bending oscillations in the presence of axial vibrations to be determined by a system of ordinary differential equations. For both light and massive rods the dynamical evolution of the system can be reduced to a study of solutions of the Mathieu-Hill equation. A stability analysis for a light rod based on this equation has been performed and its effectiveness compared with a direct numerical analysis based on period mapping techniques. The method based on the Matheiu-Hill approximation has been extended to the case of a heavy rod where a direct numerical analysis is more computationally intensive.

Acknowledgement

The authors are most grateful to S. Antman for his valuable advice on this investigation and to the Leverhulme Trust, EPSRC and BP-Amoco for financial support.

Literature

1. Antman, S.: Non-linear Problems in Elasticity.Applied Mathematical Sciences 107, Springer-Verlag, (1991).
2. Antman, S.S.; Marlow, R.S.; Vlahacos, C.P.: The complicated dynamics of heavy rigid bodies attached to deformable rods. Quarterly of Applied Mathematics, 86, (1998), 431.
3. Arnold, V.I.: Mathematical Methods of Classical Mechanics. Second Edition, Springer Verlag, (1989).
4. Cartmell, M.: Introduction to Linear, Parametric and Nonlinear Vibrations. Chapman and Hall, (1990).
5. Collatz, L.: Differential Equations: An Introduction with Applications. Wiley, (1986), 180–184.
6. Dunayevsky,V.A.; Abbassian, F.; Judziz, A.: Drilling and Completion 84-92, Dynamic Stability of Drill-strings Under Fluctuating Weight on Bit, SPE, (1993).
7. Fear, M.J.; Abbassian, F.: Experience in the Detection and Suppression of Torsional Vibration of Torsional Vibration from Mud Logging Data. SPE 28908, (1994), 433-448.
8. Mond, M.; Cederbaum, G.; Khan, P.B.; Zarmi, Y.: Stability Analysis of the Non-linear Mathieu Equation. Journal of Sound and Vibration, 167, (1993), 77.
9. Newland, D.E.: Mechanical vibration analysis and computation. Longman, (1989).
10. Quinn, T.J.; Speake, C.C.; Brown, L.M.: Phil. Mag. A65, (1992), 265.
11. Speake, C.C.; Quinn, T.J.; Davis R.S.; Richman, S.J.: Experiment and theory in anelasticity. Meas. Sci. Technol., 10, (1999), 430.
12. Timoshenko, S.P.; Gere, J.E.: Theory of Elastic Stability, McGraw-Hill, (1961).
13. Tucker, R.W.; Tung, R.S.; Wang, C.: Nonlinear Flexural Excitations and Drill-string Dynamics. Extracta Mathematicae, 14(2), (1999), 217-246.
14. Tucker, R.W.; Wang, C.: The Excitation and Control of Torsional Slip-Stick in the Presence of Axial Vibrations. http://www.lancs.ac.uk/users/SPC/Physics.htm, (1997).
15. Tucker, R.W.; Wang, C.: On the Effective Control of Torsional Vibrations in Drilling Systems. J. Sound and Vibration, 224(1), (1999a), 101-122.
16. Tucker, R.W.; Wang, C.: An Integrated Model for Drill String Dynamics. J. Sound and Vibration, 224(1), (1999b), 123-165.

Address: Dr. S.J. Cull, FMC Department, DERA Bedfort, Bedfordshire, MK41 6AE, UK, s.cull@virgin.net, Prof. R.W. Tucker, Prof. R.S. Tung, Department of Physics, Lancaster University, LA1 4YB, r.tucker@lancaster.ac.uk, r.tung@lancaster.ac.uk, Dr. D.H. Hartley, Department of Physics, University of Adelaide, Australia, DHartley@physics.adelaide.edu.au